

Smooth embeddings in contracting recurrent networks driven by regular dynamics:

A synthesis for neural representation

Vikas N. O'Reilly-Shah MD PhD¹ and Alessandro Maria Selvitella PhD^{2,3}

¹*Department of Anesthesiology & Pain Medicine, University of Washington School of Medicine, Seattle, WA, USA*

²*Department of Mathematical Sciences & Laboratory of Data Science, Purdue University Fort Wayne, Fort Wayne, IN, USA*

³*eScience Institute, University of Washington, Seattle, WA, USA*

January 24, 2026

Corresponding author: Vikas N. O'Reilly-Shah (voreill@uw.edu)

Address: RR450, 1959 NE Pacific St, Seattle, WA 98195, USA.

Data Availability Statement: This is a theoretical synthesis paper. No new data were generated or analyzed. There is no empirical data or code associated with this article.

Abstract

Recurrent neural networks trained for time-series prediction often develop latent trajectories that preserve qualitative structure of the dynamical systems generating their inputs. Recent empirical work has documented topology-preserving latent organization in trained recurrent models, and recent theoretical results in reservoir computing establish conditions under which the synchronization map is an embedding. Here we synthesize these threads into a unified account of when contracting recurrent networks yield smooth, topology-preserving internal representations for a broad and biologically relevant class of inputs: regular dynamics on invariant circles and tori.

Our contribution is an integrated framework that assembles (i) generalized synchronization and embedding guarantees for contracting reservoirs, (ii) regularity mechanisms ensuring differentiability of the synchronization map under mild constraints, and (iii) a base-system viewpoint in which the invariant manifold generating the input stream is treated as the driving system. In this regular setting, the conditions commonly viewed as restrictive in chaotic-attractor analyses become mild and readily satisfied by standard contractive architectures. The framework clarifies how representational content in recurrent circuits is inherently historical: the network state encodes finite windows of input history rather than instantaneous stimuli.

By consolidating disparate empirical and theoretical results under common assumptions, the synthesis yields concrete, testable expectations about when prediction-trained recurrent circuits should (or should not) form smooth latent embeddings and how required state dimension scales with the intrinsic dimension of the driving dynamics.

Author summary

When recurrent neural networks are trained to predict a time series, their hidden activity often appears to “recover” the structure of the dynamical system that produced the data. We explain how

and when this can happen by bringing together several lines of prior work. We focus on a common and biologically relevant case in which inputs are generated by regular dynamics, such as rotations on a circle or quasiperiodic motion on a torus. In this setting, contracting recurrent networks can synchronize to the input-driven dynamics, and the resulting mapping from the underlying system into network state can preserve geometry and topology. We assemble existing results and perspectives into a coherent framework that clarifies the assumptions required for smooth, topology-preserving latent representations. Our synthesis also highlights an important conceptual point: the network state represents recent input history, not an instantaneous stimulus. This yields practical expectations for experiments and simulations about when predictive training should produce faithful latent representations and when it should fail.

1 Introduction

1.1 Empirical Motivation: RNNs Learn Embeddings

Two recent empirical studies have demonstrated a striking phenomenon: recurrent neural networks trained to predict time series develop hidden-state dynamics that reproduce the topological structure of the underlying attractor.

Uribarri and Mindlin [1] trained Long Short-Term Memory (LSTM) networks on the x -component of the chaotic Rössler system. They found that 94% of successfully trained models produced hidden-state trajectories with correct topological organization of periodic orbits, verified by linking number analysis. Crucially, models with incorrect topology exhibited significantly higher prediction error, suggesting that accurate prediction *requires* faithful dynamical representation.

Ostrow, Eisen, and Fiete [2] compared transformers and state-space models on partially-observed dynamical systems, finding strong correlations (test $R^2 = 0.76$) between embedding quality metrics (neighbor overlap, decoder R^2 , conditional variance) and prediction performance. State-space models exhibited stronger inductive biases for embedding, achieving better attractor reconstructions with fewer parameters.

1.2 Theoretical Foundation: Generalized Synchronization

The theory of generalized synchronization (GS) may provide some insight into these empirical findings. When a recurrent network satisfying the echo state property is driven by observations from a dynamical system, the network state becomes functionally dependent on the driving system's state via a synchronization function f . Recent work by Hart [3] establishes that, under generic conditions, this synchronization function is not merely continuous but is a C^1 *embedding*: a smooth, injective map with smooth inverse.

This result connects two literatures:

- **Delay coordinate embedding** (Takens [4], Sauer–Yorke–Casdagli [5]): Observations of a dynamical system, appropriately lagged, generically yield an embedding of the underlying attractor.
- **Reservoir computing**: Recurrent networks driven by time series develop internal representations that encode input history in a manner analogous to delay coordinates.

The synthesis: trained RNNs implement delay coordinate embedding internally, with h_t encoding input history.

1.3 Perception Under The State Space Theory

The State Space Theory (SST) [6, 7] proposes that these mathematical structures are not merely useful for machine learning but describe the computational architecture of biological perception. SST advances the following hypothesis:

At the level of early sensory representation, perceptions can be modeled as *state-space embeddings* of environmentally generated dynamics into neural state space, and that perceptual structure corresponds to the invariants and geometry of those embeddings.

Accordingly, in regimes where recurrent circuits are effectively contractive under naturalistic input classes (Section 2.5), predictive learning is expected to drive representations toward (approximate) injectivity and dynamical faithfulness, making the Ostrow and Uriarri findings natural rather than anomalous.

This paper provides rigorous mathematical foundations for a candidate mechanism underlying the sensory component of SST. It establishes that, under mild conditions, recurrent networks driven by regular dynamics implement C^1 embeddings. We focus on regular dynamics because, as we argue below, they provide a clean and empirically relevant model class for many early sensory perceptual primitives, without claiming universality.

1.4 Why Regular Dynamics Matter for Perception

For applications to early sensory processing and neural representation, we do not require the full machinery of strange attractors. We adopt the modeling hypothesis that a wide class of perceptually central *effective* dynamics (after physical and neural filtering and at the timescales relevant for prediction) can often be well-approximated by regular, low-dimensional structure (invariant circles/tori and slowly varying manifolds), even though real-world signals also contain stochasticity and intermittently complex transients.

The examples below motivate this hypothesis and delineate its intended scope, without claiming that all perceptual dynamics are regular.

Motion tracking. Many canonical tracking problems are governed by low-dimensional regular dynamics: pendular motion traces a limit cycle; rotation is dynamics on S^1 ; coordinated gait and gesture are often well approximated by low-dimensional oscillatory structure. The perceptual system must represent these dynamics to predict interception, anticipate return, and track rotation [8]. These are not strange attractors; they are low-dimensional regular regimes. Even complex biological motion is frequently modeled by low-dimensional attractors [9, 10].

Auditory processing. A pure tone is a limit cycle in phase space. A chord with k incommensurate frequencies is quasiperiodic motion on a k -torus. Speech involves sequences of relatively stable attractor states (formant configurations for vowels, transient trajectories for consonants) [11, 12]. Rhythm is periodic structure [13]. Arguably, even complex music, from the perspective of what the auditory system must track for perception, involves periodic and quasiperiodic dynamics rather than chaos.

Color vision. Chromatic signals occupy a low-dimensional opponent-process space (L-M, S-(L+M), luminance) [14]. Color constancy mechanisms stabilize perception across illumination changes; the relevant dynamics is slow drift on a low-dimensional manifold, not strange attractor reconstruction [15].

Prediction error. A compatible interpretation of the embedding framework is that prediction-error minimization pressures internal states toward dynamically faithful, state-separating representations. In predictive-processing or free-energy formulations [16, 17], this is often expressed as minimizing expected prediction error (or a variational bound thereon) under an agent’s implicit

generative model. In that spirit, the synchronization map $f : M \rightarrow \mathbb{R}^N$ can be viewed as a geometric object encoding the agent’s learned dynamical model of its sensory stream. The embedding theorems then show that, in regular regimes, such representations can be realized by contracting recurrent circuits.

The key insight. Embedding regular cycles and tori is a mathematically simpler target than embedding strange attractors: the relevant domination bounds are milder and the intrinsic dimensions are small. The present framework therefore provides a principled baseline for when smooth, topology-preserving representations should be expected in recurrent circuits, without asserting that the same guarantees apply in chaotic regimes.

Regular dynamics as a deliberate “clean case.” The restriction to regular circle/torus dynamics is not intended to explain the most difficult empirical settings (e.g. strange attractors under partial observation). Rather, it isolates a regime in which the synchronization and smoothness hypotheses can be checked in simple quantitative terms and where the resulting predictions are sharp. Empirically, many sensory primitives (periodicity, phase, and quasiperiodicity) naturally live in this regime; theoretically, it provides a baseline against which more complex (chaotic, stochastic, or intermittently driven) cases can be compared.

1.5 Neural Implementation: Levels of Description

SST proposes that cortical circuits implement delay coordinate embedding, but biological neurons differ from the abstract RNN equation $h_{t+1} = F(h_t, u_t)$. Individual neurons communicate through discrete action potentials; dendritic trees perform continuous spatiotemporal integration; synaptic plasticity operates on multiple timescales. How does this biological complexity relate to the mathematical framework?

SST’s claim operates at the mesoscale: the state $h_t \in \mathbb{R}^N$ represents not individual neuron activity but low-dimensional population dynamics, the level at which neural manifolds are empirically observed [10, 18]. The observation function $\omega : M \rightarrow \mathbb{R}$ corresponds to sensory transduction: photoreceptors, hair cells, and mechanoreceptors converting physical signals to neural input. The reservoir map F is shaped by synaptic plasticity during development and perceptual learning, the biological analogue of RNN training [19–21]. Table 1 summarizes SST’s claims.

Remark 1.1 (Scope: Fixed Parameters and Asymptotic Idealization). The synchronization function $f : M \rightarrow \mathbb{R}^N$ characterized by our theorems describes networks with *fixed parameters*: the regime of trained artificial RNNs or biological circuits on timescales short relative to synaptic modification. This f should be understood as the *target* toward which plastic circuits are driven by prediction error minimization, not a literal description of any instantaneous biological state. The invariance condition $f(\phi(x)) = F(f(x), \omega(x))$ describes an ongoing dynamical relationship: the neural state $h_t = f(m_t)$ is constituted by its role in temporal evolution, not as a static snapshot.

Remark 1.2 (Bunching as a Gain–Stability Constraint Under Plasticity). The bunching condition $\rho \|D\phi^{-1}\|_{C^0(M)} < 1$ should be read as a *gain–stability* constraint for smooth representation: it requires that the effective contraction of the driven neural dynamics (quantified by $\rho := \sup \|\partial_h F\|_{\text{op}}$ on the relevant compact set) dominates the backward expansion of the environmental dynamics. Our theorems treat F as fixed, but biologically F is shaped by plasticity. Under a standard timescale-separation idealization (synaptic change slower than state evolution), plasticity can be viewed as slowly adjusting the effective gain of the circuit, thereby moving the system into (or out of) the bunching regime and inducing a slow drift of the corresponding synchronization map f . In this sense, bunching does not describe plasticity dynamics; rather, it characterizes the

Level	Mathematical Entity	Biological Interpretation
Environmental dynamics	Manifold M , diffeomorphism ϕ	Physical process being perceived (projectile motion, sound wave, reflectance spectrum)
Observation function	$\omega : M \rightarrow \mathbb{R}$	Sensory transduction (photoreceptors, cochlear hair cells, mechanoreceptors)
Input signal	$u_t = \omega(\phi^t(m_0))$	Afferent neural activity (spike-coded signal reaching cortex)

Two routes to embedding:

Delay coordinates	$\Phi_\omega^n : M \rightarrow \mathbb{R}^n$ $\Phi_\omega^n(x) = (\omega(x), \dots, \omega(\phi^{n-1}(x)))$	Explicit storage of input history (tapped delay lines); simplified/idealized motivation for SST [6]
Hidden state	$h_t \in \mathbb{R}^N$	Mesoscale population activity (firing rates, low-dimensional projection of spike patterns)
Recurrent dynamics	$F : \mathbb{R}^N \times \mathbb{R} \rightarrow \mathbb{R}^N$ $h_{t+1} = F(h_t, u_t)$	Recurrent cortical dynamics (abstracted over spiking/dendritic details)
Synchronization function	$f : M \rightarrow \mathbb{R}^N$ $f(\phi(x)) = F(f(x), \omega(x))$	The learned embedding: representation as prediction

Connection (Proposition 4.6): $f(x) \approx g_L(\Phi_\omega^L(\phi^{-L}(x)))$: the ESM encodes delay coordinates implicitly.

Table 1: Levels of description relating mathematical framework to neural implementation. Two routes yield embeddings: explicit delay coordinates (Takens) and implicit encoding via recurrent dynamics (generalized synchronization). Proposition 4.6 establishes their relationship; SST proposes that cortex primarily uses the second route.

instantaneous representational regime that plasticity can stabilize via homeostatic and predictive-learning mechanisms, without requiring global ESP to hold across all inputs or all cortical areas.

1.6 Temporal Structure in Neural Representations

The mathematical framework has structural implications for the nature of neural representations:

1. The neural state h_t encodes information equivalent to a temporal trajectory $(m_t, m_{t-\tau}, \dots, m_{t-L\tau})$, not merely the instantaneous environmental state m_t .
2. The *information content* of the representation is inherently historical: for fixed network parameters (i.e. over a perceptual episode), h_t depends on a window of past states/inputs and cannot be reconstructed from an instantaneous environmental state alone. If parameters adapt

on comparable timescales, then h_t reflects both the environmental trajectory and the learning dynamics and our theorems do not apply. The results here concern the fixed-parameter regime.

3. If perceptual experience supervenes or is constituted by such representations, this temporal structure would be reflected in the structure of experience.

These observations are compatible with, and may provide formal grounding for, process-philosophical accounts of temporal experience [22, 23]. The metaphysical interpretation of this compatibility is developed elsewhere under the framework of computational dynamic monism (CDM) [24]. Here we note only the structural parallel: the embedding framework establishes that what is *represented* is a trajectory through time, not a snapshot. Whether this entails that *experience* is constitutively temporal requires additional philosophical argument beyond the scope of this paper.

1.7 Scope and Purpose

This paper synthesizes existing mathematical results to underline that contracting RNNs generically implement C^1 embeddings when driven by regular dynamics on circles and tori. We do not claim new theorems; our contribution is assembling results from delay-coordinate embedding, generalized synchronization, and reservoir computing into a unified framework that provides mathematical foundations for theories of neural representation. The restriction to regular dynamics yields three simplifications:

1. Bunching conditions reduce to mild constraints on contraction rates.
2. Weak generalized synchronization (continuous but non-differentiable) does not arise.
3. Dimension requirements ($N > 2d$) are small and biologically plausible.

The logical structure is:

1. *Empirical findings* [1, 2]: RNNs trained on time series develop topologically correct representations.
2. *Theoretical framework* [3, 25, 26]: Generalized synchronization establishes conditions for C^1 embedding.
3. *This synthesis*: For regular dynamics, these conditions are mild.

1.8 Claims and Non-Claims

We establish: (i) Contracting RNNs driven by regular dynamics on circles/tori generically implement C^1 embeddings under mild bunching conditions. (ii) Multi-step prediction accuracy imposes a state-separation constraint: under a uniform multi-step approximation bound, the internal state must be approximately injective in the sense of Proposition 6.4. (iii) Dimension requirements ($N > 2d$) are biologically plausible.

We do not address: Training dynamics (how gradient descent or plasticity finds embeddings); chaotic attractors (the Uribarri/Ostrow settings); hierarchical integration or gain-modulated competition (central to SST's account of consciousness); or whether biological circuits satisfy ESP, though we argue input-dependent ESP is plausible for sensory cortex (Section 2.5).

1.9 Paper Organization

Section 2 establishes mathematical definitions and states background theorems. Section 3 presents the key simplification: treating the invariant manifold as the base system. Section 4 synthesizes results to characterize embeddings for regular dynamics. Section 5 discusses dimension requirements and their biological plausibility. Section 6 connects prediction objectives to embedding structure. Section 7 addresses implications for SST and limitations.

2 Mathematical Preliminaries

We establish notation and state foundational theorems.

2.1 Dynamical Systems: Discrete vs. Continuous Time

We formulate dynamics in discrete time as iterates of a smooth map. Concretely, our base dynamical system is a pair (M, ϕ) where M is a compact smooth manifold of positive dimension and $\phi : M \rightarrow M$ is a C^r diffeomorphism ($r \geq 2$). In most applications below we take $r = 2$, which is sufficient for all cited regularity and embedding results.

Here, C^r refers to regularity in the *state variable* on M ; the time index $t \in \mathbb{Z}$ is discrete and we never assume differentiability with respect to time. This discrete-time viewpoint covers both genuinely discrete systems and sampled continuous-time flows: if $\{\Phi_t\}_{t \in \mathbb{R}}$ is a C^r flow on M , then for any sampling interval $\tau > 0$ the time- τ map $\phi := \Phi_\tau$ is a C^r diffeomorphism, and the sampled trajectory $x_{t+1} = \phi(x_t)$ is a discrete-time system.

Remark 2.1 (Regularity Conditions). We track three logically distinct steps, following the cited results.

- **Existence/uniqueness of GS (continuous f):** Under $\phi \in \text{Diff}^1(M)$, ω continuous, and F at least C^1 in h , strict ESP yields a unique *continuous* synchronization map f (Theorem 2.16; cf. [26]).
- **C^1 regularity of f :** A bunching-type domination condition upgrades f to C^1 under stronger smoothness assumptions on ϕ, ω, F (Theorem 2.18; cf. [26, 27]).
- **Generic C^1 embedding:** Under $N > 2\dim(M)$ and genericity hypotheses on ω and F (within the ESP+bunching class), f is generically a C^1 embedding (Theorem 2.21; [3]). In the quasiperiodic circle/torus settings of Definition 2.4, periodic-orbit hypotheses are vacuous.

For readability we typically assume ϕ, ω, F are C^2 , which is a convenient sufficient regime for all steps above. The key conclusions we use concern the existence of a *continuous* GS map f , its upgrade to a C^1 map under bunching, and, generically, its being a C^1 *embedding*.

Remark 2.2 (Continuous-Time Origin). In applications, discrete-time maps often arise as time- τ samples of continuous flows. If $\{\Phi_t\}_{t \in \mathbb{R}}$ is a C^r flow on M (with $r \geq 1$), then for any fixed sampling interval $\tau > 0$ the time- τ map

$$\phi := \Phi_\tau : M \rightarrow M$$

is a C^r diffeomorphism. Our results apply to such sampled systems. The choice of τ affects the specific dynamics (rotation number, contraction rates) but not the structural results.

Remark 2.3 (Biological Relevance of Discrete Time). The discrete-time formulation $h_{t+1} = F(h_t, u_t)$ can be interpreted as a mesoscale sampling of underlying continuous neural dynamics: if $\{\Phi_t\}$ is a flow, then $\phi = \Phi_\tau$ is the time- τ map, and τ corresponds to a characteristic integration window for population activity. The framework permits τ on millisecond timescales, with the appropriate value depending on the circuit and task. At the population level (firing rates or low-dimensional projections), neural activity exhibits low-dimensional structure empirically [10, 18], which is the level at which the embedding statements apply.

2.2 Classes of Regular Dynamics

We distinguish several cases by the topology of the base manifold M :

Definition 2.4 (Regular Base Systems). A *regular base system* is a pair (M, ϕ) where one of the following holds:

- (i) **Invariant circle (quasiperiodic):** $M = S^1$ and $\phi : S^1 \rightarrow S^1$ is C^2 -conjugate to an *irrational* rigid rotation

$$R_\alpha : \theta \mapsto \theta + \alpha \pmod{1}, \quad \alpha \in \mathbb{R} \setminus \mathbb{Q}.$$

In particular, ϕ has no periodic points and all orbits are dense.

- (ii) **Invariant torus (quasiperiodic):** $M = T^k := \mathbb{R}^k / \mathbb{Z}^k$ and $\phi : T^k \rightarrow T^k$ is C^2 -conjugate to a translation

$$T_\alpha : \theta \mapsto \theta + \alpha \pmod{\mathbb{Z}^k}, \quad \alpha \in \mathbb{R}^k,$$

with $\{1, \alpha_1, \dots, \alpha_k\}$ rationally independent (so the translation is minimal / quasiperiodic).

Remark 2.5 (Strength of the conjugacy restriction). Definition 2.4 deliberately restricts to a near-isometric quasiperiodic regime by assuming C^2 conjugacy to a rigid rotation/translation. This is a strong hypothesis (not generic among all circle/torus diffeomorphisms) adopted to keep the synthesis in a clean setting where $\|D\phi^{-1}\|_{C^0(M)}$ is quantitatively controlled.

Remark 2.6 (Finite-horizon tasks via phase augmentation). Finite-horizon episodes (e.g. ballistic flight segments) can be placed into a compact recurrent setting by augmenting state with a task-phase variable $\theta \in S^1$, yielding $\tilde{M} = M \times S^1$ and an augmented map $\tilde{\phi}(x, \theta) = (\phi_\theta(x), \theta + \alpha \pmod{1})$. In this representation, a finite episode is a segment of an orbit on \tilde{M} , restoring compactness/recurrence assumptions without changing the local dynamical content being modeled.

Remark 2.7 (From Ambient Dynamics to Intrinsic Structure). Regular base systems often arise as invariant manifolds within larger ambient spaces. For instance, a pendulum's state space is \mathbb{R}^2 (angle and velocity), but stable oscillation confines trajectories to a limit cycle homeomorphic to S^1 ; its intrinsic dynamics is then a regular base system in sense (i). Similarly, a complex tone with k incommensurate frequencies traces a trajectory on a k -torus embedded in higher-dimensional acoustic/neural space.

For SST, this observation is methodologically important: the perceptual system may not need to represent the full ambient dynamics but rather only the effective low-dimensional structure carrying predictively relevant information. Our approach formalizes this by treating the invariant manifold *itself* as the base system, which yields cleaner dimension bounds and milder bunching conditions than would arise from analyzing the ambient system directly.

2.3 Delay-Coordinate Embeddings

Definition 2.8 (Delay Map). Given (M, ϕ) , an observation function $\omega : M \rightarrow \mathbb{R}$, and embedding dimension $n \in \mathbb{N}$, the *delay map* is

$$\Phi_\omega^n : M \rightarrow \mathbb{R}^n, \quad \Phi_\omega^n(x) = (\omega(x), \omega(\phi(x)), \dots, \omega(\phi^{n-1}(x))).$$

Theorem 2.9 (Takens [4]). *Let M be a compact m -dimensional manifold and $\phi \in \text{Diff}^2(M)$. Suppose:*

- (a) ϕ has finitely many periodic orbits.
- (b) For each periodic orbit of period p , the eigenvalues of $D\phi^p$ at any point on the orbit are distinct.

Then for $n \geq 2m + 1$, a generic $\omega \in C^2(M, \mathbb{R})$ yields a delay map Φ_ω^n that is a C^1 embedding.

Remark 2.10 (Periodic-orbit hypotheses are vacuous in our setting). In the quasiperiodic cases of Definition 2.4 (irrational rotation on S^1 and rationally independent translations on T^k), the map ϕ has *no periodic orbits*. Hence any hypotheses in Takens- or Hart-type embedding theorems that impose conditions on periodic orbits are satisfied vacuously here.

Theorem 2.11 (Sauer–Yorke–Casdagli [5]). *Let $\mathcal{A} \subset \mathbb{R}^{m_0}$ be a compact set with box-counting dimension $d_{\mathcal{A}}$. For $n > 2d_{\mathcal{A}}$, a prevalent set of smooth observation functions ω yields a delay map that is injective on \mathcal{A} .*

This theorem applies to sets (not just manifolds) and uses box dimension. For a k -dimensional torus, $d_{\mathcal{A}} = k$, so $n > 2k$ suffices.

2.4 Recurrent Neural Networks as Driven Systems

Consider a discrete-time RNN with hidden state $h_t \in \mathbb{R}^N$ receiving scalar input u_t :

$$h_{t+1} = F(h_t, u_t), \tag{1}$$

where $F : \mathbb{R}^N \times \mathbb{R} \rightarrow \mathbb{R}^N$ is C^2 . When the input derives from observing a dynamical system ($u_t = \omega(\phi^t(x_0))$ for initial condition $x_0 \in M$) the RNN becomes a *skew-product* system:

$$\Psi : M \times \mathbb{R}^N \rightarrow M \times \mathbb{R}^N, \quad \Psi(x, h) = (\phi(x), F(h, \omega(x))).$$

Definition 2.12 (Echo State Property). The RNN satisfies the *echo state property* (ESP) with contraction rate $\rho < 1$ on compact input set $U \subset \mathbb{R}$ if there exists a compact set $K \subset \mathbb{R}^N$ such that:

- (i) $F(K, u) \subseteq K$ for all $u \in U$ (forward invariance).
- (ii) $\sup_{(h,u) \in K \times U} \|\partial_h F(h, u)\|_{\text{op}} \leq \rho$ (uniform contraction).

Remark 2.13 (Architecture dependence and when ESP is plausible). ESP is a property of the *state update* $h \mapsto F(h, u)$ on the relevant compact region K and input set U . It holds, for example, for:

- **Linear reservoirs:** $F(h, u) = Wh + Bu$ with $\|W\|_{\text{op}} < 1$ (take K forward invariant).
- **Standard “tanh” RNNs:** $F(h, u) = \sigma(Wh + Bu + b)$ where σ is 1-Lipschitz and $\|W\|_{\text{op}} < 1$.

- **Gated RNNs (GRU/LSTM):** although not uniformly contractive in general, they can be contractive on the trained operating region (input-dependent or local ESP), particularly when gates enforce effective damping.

Biologically, strict *uniform* ESP across all inputs is a strong assumption; we use it as a clean sufficient condition for the GS/embedding theorems, while viewing “input-dependent” or local contractive regimes as the more plausible interpretation for sensory cortex (Section 2.5) and some thoughts on how to bridge these ideas conceptually to additional RNN regimes in Section 6.

2.5 Beyond Strict ESP: Biological Plausibility

Definition 2.12 requires uniform contraction across all inputs. Biological neural circuits likely violate this: cortical networks operate near criticality [28, 29], prefrontal circuits exhibit attractor dynamics and persistent activity [30–32], and intrinsic timescales vary systematically across cortex [33].

However, weaker conditions may suffice. *Input-dependent ESP* [34, 35] requires only that structured inputs—such as natural sensory signals—induce effective contraction, even if the spectral radius exceeds unity. Empirical evidence supports this for sensory cortex: V1 exhibits fading memory with ~ 100 –300 ms timescales [36], stimulus onset quenches variability [37], and population responses satisfy smoothness constraints consistent with contractivity [38].

The evidence suggests a regime-dependent picture: sensory cortex (V1, A1, S1) plausibly satisfies input-dependent ESP for natural stimuli; prefrontal cortex likely does not. Since SST locates consciousness at hierarchically high levels, the present framework-restricted to the ESP regime—addresses the *sensory front-end* of SST, not the neural correlates of consciousness proper. Extending to beyond-ESP regimes remains open.

Remark 2.14 (Beyond strict ESP). Several input-dependent or local variants of ESP have been proposed in the reservoir computing literature (e.g. contraction only along a structured input class). Such conditions may better match biological sensory circuits. In this paper, however, all formal statements use the strict ESP hypothesis (Definition 2.12) as a clean sufficient condition; we do not attempt to re-prove the GS/regularity/embedding results under weaker notions of ESP.

2.6 Generalized Synchronization

Definition 2.15 (Generalized Synchronization). The driven system Ψ exhibits *generalized synchronization* (GS) on M if there exists a continuous function $f : M \rightarrow \mathbb{R}^N$ such that:

(i) **Invariance:** $f(\phi(x)) = F(f(x), \omega(x))$ for all $x \in M$.

(ii) **Attraction:** For any $x_0 \in M$ and any initial $h_0 \in K$,

$$\|h_t - f(\phi^t(x_0))\| \rightarrow 0 \quad \text{as } t \rightarrow \infty.$$

The function f is the *synchronization function* or *echo state map* (ESM).

Theorem 2.16 (GS Existence [26]). *Let (M, ϕ) be a base system with $\phi \in \text{Diff}^1(M)$, and let $\omega : M \rightarrow \mathbb{R}$ be continuous with $U = \omega(M)$ compact. If the RNN satisfies ESP with rate $\rho < 1$ on U , then there exists a unique continuous synchronization function $f : M \rightarrow \mathbb{R}^N$. Convergence is exponential: $\|h_t - f(\phi^t(x_0))\| = O(\rho^t)$.*

Remark 2.17 (Role of the Observation Function ω). The observation function $\omega : M \rightarrow \mathbb{R}$ plays two distinct roles in the framework:

- (i) **Physical/sensory transduction:** ω models the process by which environmental states become neural inputs, e.g. photoreceptors converting light to spike rates, cochlear hair cells converting pressure waves to auditory nerve activity, etc. The choice of ω reflects which aspects of environmental dynamics are accessible to the perceptual system.
- (ii) **Mathematical constraint on embedding:** The synchronization function f and its regularity depend on ω through the invariance relation $f(\phi(x)) = F(f(x), \omega(x))$. Genericity results (Theorem 2.21) assert that for “most” observation functions, f is an embedding; pathological ω (e.g., constant functions) trivially fail. The genericity hypothesis formalizes the intuition that “typical” sensory transduction does not destroy dynamical structure.

In the commutative diagram (Figure 1), ω appears as the green arrow feeding current environmental information into the neural update; the embedding f then encodes the accumulated history in a form compatible with this input stream.

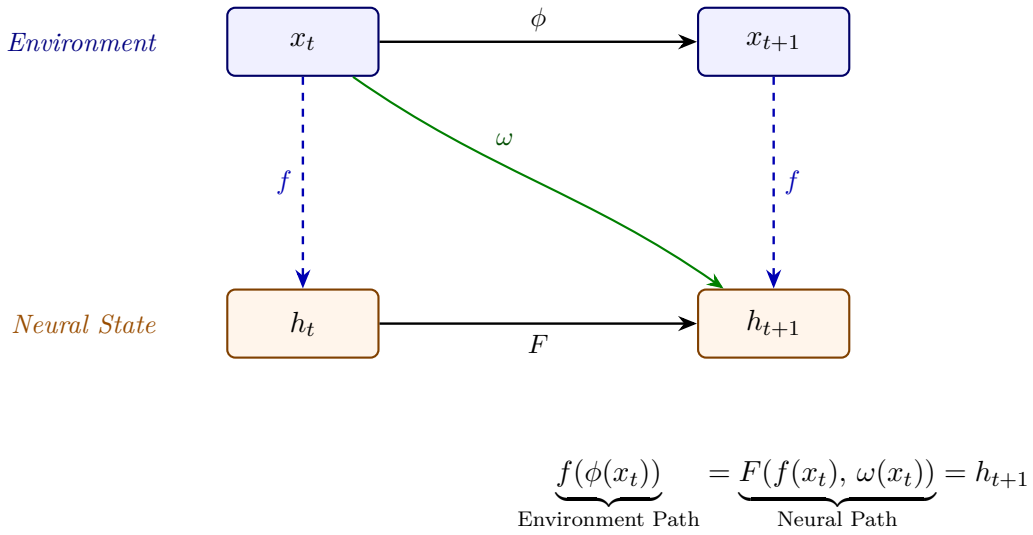


Figure 1: **Generalized synchronization as a commutative diagram.** The environment evolves via ϕ (top); the neural state evolves via the recurrent map F (bottom). The synchronization function $f : M \rightarrow \mathbb{R}^N$ (dashed blue) embeds environmental states into neural state space. The observation function $\omega : M \rightarrow \mathbb{R}$ (green) provides sensory input to the recurrent dynamics. *Commutativity* implies that evolving the environmental state and then embedding it (Environment Path) yields the same result as embedding the current state and evolving it via the neural dynamics driven by observation (Neural Path). This condition $f(\phi(x)) = F(f(x), \omega(x))$ defines the embedding.

2.7 Regularity of the Synchronization Function

The synchronization function f is always continuous when ESP holds. Obtaining C^1 regularity requires an additional *bunching condition*.

Theorem 2.18 (Regularity under Bunching [26, 27]). *Under the hypotheses of Theorem 2.16, suppose additionally that $\phi \in \text{Diff}^2(M)$, $\omega \in C^1(M, \mathbb{R})$, $F \in C^2(\mathbb{R}^N \times \mathbb{R}, \mathbb{R}^N)$, and the bunching condition holds:*

$$\rho \cdot \|D\phi^{-1}\|_{C^0(M)} < 1, \tag{2}$$

where $\|D\phi^{-1}\|_{C^0(M)} = \sup_{x \in M} \|D_x \phi^{-1}\|_{op}$. Then the synchronization function $f : M \rightarrow \mathbb{R}^N$ is C^1 .

Remark 2.19 (The Bunching Condition). Condition (2) requires the RNN’s contraction to dominate the base system’s backward expansion. For chaotic systems, $\|D\phi^{-1}\|$ can be large (exponentially growing in time for trajectories), making bunching hard to satisfy. This is where regular dynamics simplifies matters, as we develop in Section 3.

Remark 2.20 (Where contraction and expansion live). In the skew-product $\Psi(x, h) = (\phi(x), F(h, \omega(x)))$, the ESP constant ρ controls contraction in the *fiber/response variable* h (i.e. the Jacobian $\partial_h F$), while $\|D\phi^{-1}\|_{C^0(M)}$ controls backward expansion in the *base/state variable* $x \in M$. Thus the bunching inequality $\rho \cdot \|D\phi^{-1}\|_{C^0(M)} < 1$ is a quantitative domination condition: fiber contraction must dominate base backward expansion. In particular, nothing in the bunching condition asserts that the base dynamics ϕ is contracting; it may be isometric (rotations/translations) or even expanding in forward time.

2.8 Generic Embeddings

Theorem 2.21 (Generic Embeddings [3]). *Let (M, ϕ) be a base system with M a compact m -dimensional manifold and $\phi \in \text{Diff}^2(M)$ satisfying:*

- (a) *ϕ has finitely many periodic orbits.*
- (b) *For each periodic orbit of period p , the m eigenvalues of $D\phi^p$ (at any point on the orbit) are pairwise distinct. NB: in the quasiperiodic circle/torus cases considered here there are no periodic orbits, so Hart’s periodic-orbit nondegeneracy conditions are vacuous.*

Suppose $N > 2m$. Then for generic $\omega \in C^1(M, \mathbb{R})$ and generic reservoir maps F (among those satisfying ESP and the bunching condition), the synchronization function $f : M \rightarrow \mathbb{R}^N$ is a C^1 embedding.

This theorem combines Whitney-type genericity (embeddings are generic in $C^1(M, \mathbb{R}^N)$) with the GS machinery.

Remark 2.22 (Genericity in function spaces). Theorem 2.21 is stated for generic ω in $C^1(M, \mathbb{R})$. Since $C^2(M, \mathbb{R}) \subset C^1(M, \mathbb{R})$ is dense, we interpret “generic ω ” in this paper as generic within the relevant regularity class being used (and we assume $\omega \in C^2$ only to streamline other smoothness requirements). When needed, one may replace $\omega \in C^2$ by $\omega \in C^1$ throughout, at the expense of matching regularity hypotheses across the cited results.

3 The Key Simplification: Base System as Invariant Manifold

The central insight enabling our synthesis is to treat the invariant manifold (circle or torus) as the base dynamical system, rather than as an attractor embedded in a higher-dimensional ambient space.

Motivating example (illustrative): oscillatory sensory primitives. Many sensory primitives are well-approximated, over task-relevant timescales, by low-dimensional oscillatory or quasiperiodic structure: a dominant cycle (effective S^1) or a small collection of incommensurate phases (effective T^k). Although the ambient sensory stream is high-dimensional, biophysical filtering and predictive objectives can yield an effective low-dimensional state description that carries the predictively relevant invariants for downstream computation.

Our framework formalizes this extraction: rather than analyzing how a neural network embeds a strange attractor in \mathbb{R}^{100} , we ask how it embeds the relevant invariant circle or torus that carries

the predictively useful dynamical information. This yields cleaner dimension bounds ($N > 2d$ where d is the intrinsic dimension of the invariant manifold, not the ambient space) and milder bunching conditions (Proposition 3.1).

3.1 Bunching for Regular Base Systems

Proposition 3.1 (Near-Isometric Bounds for Regular Bases). *Let (M, ϕ) be a regular base system (Definition 2.4).*

(i) *If ϕ is a rigid rotation on S^1 or rigid translation on T^k , then $\|D\phi^{-1}\|_{C^0(M)} = 1$ (so one may take $\kappa = 1$).*

(ii) *If ϕ is C^2 -conjugate to a rigid rotation/translation via a diffeomorphism $h : M \rightarrow M$, then*

$$\|D\phi^{-1}\|_{C^0(M)} \leq \|Dh\|_{C^0(M)} \|Dh^{-1}\|_{C^0(M)}.$$

In particular, in these regular regimes the bunching condition reduces to the quantitative inequality $\rho < 1/\kappa$ with $\kappa := \|D\phi^{-1}\|_{C^0(M)}$ (or any explicit upper bound on it).

Remark 3.2 (Bunching in the regular circle/torus cases). If ϕ is *exactly* a rigid rotation on S^1 or a rigid translation on T^k (with its standard flat metric), then $\|D\phi^{-1}\|_{C^0(M)} = 1$ and the bunching inequality reduces to $\rho < 1$, i.e. no restriction beyond strict ESP.

If instead ϕ is only C^2 -conjugate to a rigid rotation/translation via h (Definition 2.4), then $\|D\phi^{-1}\|_{C^0(M)}$ is controlled by the distortion constant $\kappa := \|Dh\|_{C^0(M)} \|Dh^{-1}\|_{C^0(M)}$ (Proposition 3.1), and bunching reduces to $\rho < 1/\kappa$. Thus bunching is quantitatively mild precisely in the near-isometric regime where κ is not large.

Proof. (i) Rigid rotation $R_\alpha : \theta \mapsto \theta + \alpha$ on S^1 has $DR_\alpha = 1$ everywhere (the identity on the 1-dimensional tangent space). Thus $DR_\alpha^{-1} = 1$, and $\|D\phi^{-1}\|_{C^0} = 1$. Similarly for translations on T^k .

(ii) If $\phi = h \circ R_\alpha \circ h^{-1}$, then $\phi^{-1} = h \circ R_\alpha^{-1} \circ h^{-1}$. By the chain rule, for any $x \in M$:

$$D_x \phi^{-1} = D_{R_\alpha^{-1}(h^{-1}(x))} h \cdot D_{h^{-1}(x)} R_\alpha^{-1} \cdot D_x h^{-1}.$$

Since $DR_\alpha^{-1} = \text{Id}$ (rigid rotation), this reduces to

$$D_x \phi^{-1} = D_{R_\alpha^{-1}(h^{-1}(x))} h \cdot D_x h^{-1}.$$

Taking operator norms and suprema over $x \in M$:

$$\|D\phi^{-1}\|_{C^0(M)} \leq \|Dh\|_{C^0(M)} \cdot \|Dh^{-1}\|_{C^0(M)}.$$

□

Remark 3.3 (The ‘Near-Isometric’ Regime). For C^2 -conjugate rotations, $\kappa := \|Dh\|_{C^0} \cdot \|Dh^{-1}\|_{C^0}$ is the condition number of the conjugacy. If the conjugacy is close to the identity (mild distortion), κ is close to 1. The bunching condition $\rho \cdot \|D\phi^{-1}\| < 1$ then requires only $\rho < 1/\kappa$, which is satisfied for sufficiently contracting RNNs. Unlike chaotic systems where bunching can require extremely small ρ , here the constraint is mild.

3.2 Numerical Example: Quantitative Bunching in a Quasiperiodic Regime

We illustrate the bunching condition (2) with a concrete (purely illustrative) parameter choice in a quasiperiodic setting.

Setup. Let the base be a rigid translation on the 2-torus $T^2 = \mathbb{R}^2/\mathbb{Z}^2$,

$$\phi(\theta_1, \theta_2) = (\theta_1 + \alpha_1, \theta_2 + \alpha_2) \pmod{\mathbb{Z}^2},$$

with rationally independent $\alpha_1 = 1/\sqrt{2}$ and $\alpha_2 = 1/\sqrt{3}$. With the standard flat metric, $D\phi \equiv I$, hence $\|D\phi^{-1}\|_{C^0(T^2)} = 1$ and one may take $\kappa = 1$.

Reservoir parameters (operator-norm control). Consider a standard “tanh” RNN

$$h_{t+1} = \tanh(Wh_t + W^{\text{in}}u_t + b).$$

Since \tanh is 1-Lipschitz and $\|\tanh'(z)\| \leq 1$ pointwise, the fiber Jacobian satisfies

$$\|\partial_h F(h, u)\|_{\text{op}} \leq \|W\|_{\text{op}} \quad \text{for all } (h, u).$$

Thus, a clean sufficient condition for strict ESP (Definition 2.12) is $\|W\|_{\text{op}} < 1$ (after restricting to a forward-invariant compact K). One way to ensure this transparently is to take

$$W = sQ, \quad 0 < s < 1,$$

with Q orthogonal, so that $\|W\|_{\text{op}} = s$ exactly. Choosing, for instance, $s = 0.95$ yields an ESP contraction rate $\rho \leq 0.95$. (Importantly, this uses $\|W\|_{\text{op}}$ directly; for non-normal W , the spectral radius $\rho(W)$ alone does not control contraction.)

Bunching verification. With $\kappa = 1$ and $\rho \leq 0.95$,

$$\rho \|D\phi^{-1}\|_{C^0} \leq 0.95 \cdot 1 = 0.95 < 1,$$

so the bunching condition (2) holds with a $\sim 5\%$ margin. In this rigid quasiperiodic case, bunching imposes no constraint beyond strict ESP, consistent with Proposition 3.1.

Conjugacy distortion (upper-bound form). If instead ϕ is only C^2 -conjugate to a rigid translation via h (Definition 2.4), then Proposition 3.1 gives the upper bound

$$\|D\phi^{-1}\|_{C^0(M)} \leq \kappa := \|Dh\|_{C^0(M)} \|Dh^{-1}\|_{C^0(M)}.$$

For a moderate distortion level, say $\kappa = 1.05$, bunching requires $\rho < 1/\kappa \approx 0.952$, which is still met by the choice $\rho \leq 0.95$ above. This illustrates the intended “near-isometric” regime: as long as κ is not large, bunching remains quantitatively mild.

Dimension requirements. For T^2 ($d = 2$), Theorem 4.3 requires $N > 2d = 4$; see Section 5 for a dedicated discussion of dimension bounds and their interpretation.

Interpretation. In quasiperiodic circle/torus regimes, bunching reduces to an explicit domination inequality between (i) an operator-norm contraction bound in the driven network and (ii) a near-isometric bound on backward expansion of the base. In particular, for rigid rotations/translations ($\kappa = 1$), bunching is effectively “no stronger than fiber contraction” (strict ESP), and for C^2 -conjugate near-isometries it remains mild provided κ stays close to 1. For discussion of biological evidence for regime-dependent (input-dependent) stability and fading-memory behavior in cortex, see Section 2.5.

3.3 Avoiding Weak Generalized Synchronization

To delineate the scope of our C^1 conclusions, we note that for chaotic driving systems, the synchronization function can exist but fail to be differentiable: so-called *weak* generalized synchronization [39]. This occurs when bunching fails: the drive’s expansion overwhelms the response’s contraction.

Proposition 3.4 (No Weak GS for Regular Bases). *For a regular base system with $\|D\phi^{-1}\|_{C^0(M)} \leq \kappa$, if the RNN satisfies ESP with rate $\rho < 1/\kappa$, then the synchronization function is C^1 . Weak (non-smooth) GS does not arise.*

Proof. Proposition 3.1 shows the bunching condition is satisfied. Theorem 2.18 then guarantees C^1 regularity. \square

4 Main Results: Synthesis

We now state the synthesized results, combining the framework of Section 3 with the background theorems.

Assumption 4.1 (Standard Setup). Throughout this section:

(A1) (M, ϕ) is a regular base system (Definition 2.4) with M a d -dimensional manifold ($d = 1$ for circle, $d = k$ for k -torus).

(A2) $\phi \in \text{Diff}^2(M)$ and there exists a constant $\kappa \geq 1$ such that

$$\|D\phi^{-1}\|_{C^0(M)} := \sup_{x \in M} \|D_x\phi^{-1}\|_{\text{op}} \leq \kappa.$$

(A3) The observation function $\omega : M \rightarrow \mathbb{R}$ is C^2 .

(A4) The RNN $F : \mathbb{R}^N \times \mathbb{R} \rightarrow \mathbb{R}^N$ is C^2 and satisfies ESP with rate $\rho < 1/\kappa$.

(A5) $N > 2d$.

Remark 4.2 (Interpreting κ in Regular Regimes). If ϕ is a rigid rotation on S^1 or a rigid translation on T^k , then $\|D\phi^{-1}\|_{C^0(M)} = 1$, so one may take $\kappa = 1$. More generally, if $\phi = h \circ R \circ h^{-1}$ is C^2 -conjugate to a rigid rotation/translation R via a diffeomorphism h , then

$$\|D\phi^{-1}\|_{C^0(M)} \leq \|Dh\|_{C^0(M)} \|Dh^{-1}\|_{C^0(M)},$$

so Assumption 4.1(A2) holds with κ equal to the conjugacy condition number.

Theorem 4.3 (Embedding for Regular Base Systems). *Under Assumption 4.1:*

(i) *There exists a unique C^1 synchronization function $f : M \rightarrow \mathbb{R}^N$.*

(ii) For generic ω and generic F (among those satisfying (A4)), the map f is a C^1 embedding.

(iii) (**Induced dynamics, conditional.**) If f is injective, then the dynamics on $f(M)$ are conjugate to ϕ via

$$\psi := f \circ \phi \circ f^{-1} : f(M) \rightarrow f(M),$$

so that $\psi \circ f = f \circ \phi$. If, moreover, f is a C^1 embedding (as in (ii)), then $f : M \rightarrow f(M)$ is a C^1 diffeomorphism onto its embedded image and ψ is a C^1 diffeomorphism of the embedded submanifold $f(M)$. By invariance one has $\psi(z) = F(z, \omega(f^{-1}(z)))$ for all $z \in f(M)$.

Proof. (i) By Theorem 2.16, Assumption 4.1(A4) (ESP on $U = \omega(M)$) implies existence and uniqueness of a continuous synchronization function $f : M \rightarrow \mathbb{R}^N$ satisfying

$$f(\phi(x)) = F(f(x), \omega(x)) \quad \forall x \in M,$$

and exponential tracking of the invariant graph (as stated in Theorem 2.16). Moreover, Assumption 4.1(A2)–(A4) gives

$$\rho \cdot \|D\phi^{-1}\|_{C^0(M)} \leq \rho \kappa < 1,$$

so the bunching condition (2) holds and Theorem 2.18 upgrades f to C^1 .

(ii) In the quasiperiodic cases of Definition 2.4, ϕ has no periodic points, hence the periodic-orbit hypotheses in Theorem 2.21 are vacuous (cf. Remark 2.10). With $N > 2d$ (Assumption 4.1(A5)), Theorem 2.21 applies, giving that for generic ω and generic F (among those satisfying ESP and bunching), the synchronization function f is a C^1 embedding.

(iii) Assume f is injective. Since M is compact and $f(M) \subset \mathbb{R}^N$ is Hausdorff, the continuous bijection $f : M \rightarrow f(M)$ is a homeomorphism; in particular, $f^{-1} : f(M) \rightarrow M$ is continuous. Thus

$$\psi := f \circ \phi \circ f^{-1} : f(M) \rightarrow f(M)$$

is well-defined and continuous, and it satisfies $\psi \circ f = f \circ \phi$. If, moreover, f is a C^1 embedding, then f^{-1} is C^1 and ψ is a C^1 diffeomorphism of the embedded submanifold $f(M)$. Finally, for $z \in f(M)$, writing $z = f(x)$ with $x = f^{-1}(z)$, the invariance relation yields

$$\psi(z) = f(\phi(x)) = F(f(x), \omega(x)) = F(z, \omega(f^{-1}(z))),$$

as claimed. \square

Remark 4.4 (Comparison to Chaotic Attractors). For chaotic systems, bunching may fail and the synchronization function may be only Hölder continuous. Our synthesis does not explain the Uribarri/Ostrow findings directly but establishes that embedding is easier for regular systems.

Remark 4.5 (Uniqueness and Perceptual Multistability). The uniqueness of the synchronization function f in Theorem 4.3(i) is a consequence of the *uniform* contraction assumed in our ESP hypothesis: within the specified compact region K and input range $U = \omega(M)$, all driven trajectories converge to a single invariant graph.

Many phenomena discussed in the perception literature, including perceptual multistability under ambiguous stimuli (e.g. Necker cube, binocular rivalry), are naturally modeled by dynamics with *multiple* attracting sets or competing metastable states, in which the expressed percept depends on history and initial conditions. Such behavior is not captured by the uniformly contractive, single-graph regime analyzed here, and would require relaxing the global ESP/bunching assumptions (e.g.

allowing non-contractive or locally contractive dynamics, or explicit competitive/attractor-network mechanisms). Accordingly, the present framework is best interpreted as characterizing a stable, input-driven regime of sensory processing; extending the analysis to multistable regimes remains an important direction beyond our scope (Section 2.5).

4.1 Relation to Delay Coordinates

Proposition 4.6 (Finite-Lag Approximation [26]). *Under Assumption 4.1, for any $\varepsilon > 0$ there exists $L \in \mathbb{N}$ and a continuous $g_L : \mathbb{R}^L \rightarrow \mathbb{R}^N$ such that*

$$\sup_{x \in M} \|f(x) - g_L(\omega(\phi^{-L}(x)), \dots, \omega(\phi^{-1}(x)))\| < \varepsilon.$$

The error decays as $O(\rho^L)$.

This shows the ESM is approximately a function of a delay vector, connecting RNN embeddings to Takens-style delay coordinates.

5 Dimension Requirements and Perceptual State Spaces

Theorem 4.3 requires $N > 2d$ where $d = \dim M$. Since $N \in \mathbb{N}$, this is equivalent to $N \geq 2d + 1$. For concrete cases:

- Circle ($d = 1$): $N \geq 3$
- 2-torus ($d = 2$): $N \geq 5$
- k -torus ($d = k$): $N \geq 2k + 1$

We examine what this implies for the neural circuits posited by SST.

5.1 Perceptual State Spaces Under SST

Section 1.4 argued that the environmental dynamics relevant to biological perception (motion trajectories, acoustic oscillations, chromatic signals) is predominantly regular and low-dimensional. We now connect this observation to the dimension bounds established in Theorem 4.3.

Conjecture 5.1 (SST Dimension Requirements). *For each sensory modality, cortical circuits processing that modality have effective dimensionality N sufficient to embed the environmental dynamics characteristic of that domain, i.e., $N > 2d$ where d is the intrinsic dimension of the relevant environmental state space.*

Table 2 summarizes the dimensional requirements implied by the perceptual domains analyzed in Section 1.4. Periodic motion and pure tones require only $N > 2$; complex tones and polyrhythms on T^k require $N > 2k$; the most demanding cases (rich timbres with $k \leq 5$ salient harmonics) require $N > 10$.

Summary. For *single low-dimensional dynamical primitives* (single rhythms, tones, rotations, or isolated tracking tasks), the embedding requirements are modest, and values like $N \lesssim 10$ already cover many canonical examples. More complex perception should be viewed as coupling and composition of multiple such primitives and modalities, which can raise the effective intrinsic dimension and therefore the required N . These constraints are easily satisfied by the neural manifold dimensionalities observed empirically (Section 5.2).

Perceptual Domain	Environmental Dynamics	Latent d	Required N
Simple periodic motion / rotation	Circle (S^1)	1	> 2
Gait with a dominant cycle	Limit cycle (intrinsic S^1)	1	> 2
Pure tone (pitch)	Circle (S^1)	1	> 2
Complex tone / chords	Torus (T^k , $k \leq 5$)	≤ 5	> 10
Simple rhythm	Circle (S^1)	1	> 2
Polyrhythm	Torus (T^k , $k \leq 3$)	≤ 3	> 6
Color opponent space (slow adaptation)	Slow manifold in \mathbb{R}^3	≤ 3	> 6

Table 2: Dimension requirements for embedding perceptual state spaces under SST.

The column “Latent d ” represents the intrinsic dimension of the environmental dynamics; “Required N ” is the minimum hidden dimension for generic C^1 embedding ($N > 2d$).

5.2 Biological Plausibility

SST proposes that cortical circuits implement embeddings at the mesoscale level of population activity Section 1.5. The dimension N corresponds not to neuron count but to the effective dimensionality of neural state space: the number of degrees of freedom in population activity patterns.

Empirical studies of neural population dynamics support the view that cortical representations are low-dimensional:

- Motor cortex population activity during reaching tasks lies on manifolds of dimension $\approx 10\text{--}15$ [18].
- Visual cortex responses to natural images can be effectively approximated by low-dimensional ($N \approx 10\text{--}20$) projections [38].
- Prefrontal dynamics during working memory tasks evolve on low-dimensional manifolds [40].

These empirically observed dimensionalities ($N \approx 10\text{--}20$) comfortably exceed the embedding requirements ($N > 2d$ for $d \leq 5$) predicted by SST for perception of regular environmental dynamics. The dimensional constraints from embedding theory are not biologically prohibitive; they are satisfied by the neural state spaces that cortical circuits empirically exhibit.

A generic sufficiency bound. The embedding framework provides a principled *generic* dimension requirement: for a d -dimensional manifold, embeddings into \mathbb{R}^N are guaranteed (under the cited hypotheses) when $N > 2d$. Equivalently, for fixed N , one expects generic embedding guarantees up to intrinsic dimension approximately $(N - 1)/2$. This should be read as a sufficient-condition scaling law, not as a hard impossibility bound for specially structured systems.

6 Prediction and Identifiability: Bridge to Other RNN Regimes

This section provides a bridge to empirical work on trained recurrent predictors (e.g. Uribarri-Mindlin [1]; Ostrow et al. [2]). Sections 4–5 analyze the strict-ESP generalized-synchronization regime and yield a smooth synchronization/embedding map under bunching. Here we record a complementary deterministic point:

If a representation supports uniformly accurate multi-step prediction of future observations, then it must be (approximately) state-separating.

This is a direct consequence of classical delay-embedding theory (Takens; Sauer–Yorke–Casdagli): for sufficiently long horizons, the forward observation map is generically injective, so any predictor that reconstructs those futures from an internal state must implicitly separate distinct underlying states. None of the theorems above depend on this section; it is included to clarify why “prediction-trained” RNNs are pressured toward injective internal representations even outside strict-ESP assumptions.

6.1 The Forward Observation Map

Definition 6.1 (K -Step Forward Map). For $K \in \mathbb{N}$:

$$\Gamma_K : M \rightarrow \mathbb{R}^{K+1}, \quad \Gamma_K(x) = (\omega(x), \omega(\phi(x)), \dots, \omega(\phi^K(x))).$$

Lemma 6.2. Under the hypotheses of Takens’ theorem (or Sauer–Yorke–Casdagli), for K sufficiently large ($K \geq 2d$ where $d = \dim M$) and generic ω , the map Γ_K is injective on M .

6.2 Prediction Implies Approximate Injectivity

Suppose an RNN is trained to predict future observations. A predictor $P : \mathbb{R}^N \rightarrow \mathbb{R}^{K+1}$ is trained to approximate $\Gamma_K \circ f^{-1}$.

Definition 6.3 (Separation modulus). Let $g : M \rightarrow \mathbb{R}^p$ be continuous on compact M . A *separation modulus* for g is any nondecreasing function $\eta : (0, \text{diam}(M)] \rightarrow (0, \infty)$ such that for all $x, x' \in M$,

$$d_M(x, x') \geq \delta \implies \|g(x) - g(x')\| \geq \eta(\delta).$$

Any continuous injective g admits a (positive) separation modulus on compact M .

Proposition 6.4 (Prediction–separation link). Let $f : M \rightarrow \mathbb{R}^N$ be the synchronization map (Definition 2.15). Fix $K \in \mathbb{N}$ and define

$$\Gamma_K(x) := (\omega(x), \omega(\phi(x)), \dots, \omega(\phi^K(x))).$$

Assume Γ_K has a separation modulus η , and let $P : \mathbb{R}^N \rightarrow \mathbb{R}^{K+1}$ satisfy the uniform error bound

$$\sup_{x \in M} \|P(f(x)) - \Gamma_K(x)\| \leq \varepsilon,$$

with $\varepsilon > 0$. Then for every $\delta > 0$ such that $2\varepsilon < \eta(\delta)$, one has

$$f(x) = f(x') \implies d_M(x, x') < \delta.$$

Proof. Assume $f(x) = f(x')$. Then $P(f(x)) = P(f(x'))$. By the uniform error bound,

$$\|P(f(x)) - \Gamma_K(x)\| \leq \varepsilon \quad \text{and} \quad \|P(f(x')) - \Gamma_K(x')\| \leq \varepsilon.$$

Hence, by the triangle inequality,

$$\begin{aligned} \|\Gamma_K(x) - \Gamma_K(x')\| &\leq \|\Gamma_K(x) - P(f(x))\| + \|P(f(x)) - P(f(x'))\| + \|P(f(x')) - \Gamma_K(x')\| \\ &\leq \varepsilon + 0 + \varepsilon = 2\varepsilon. \end{aligned}$$

Let $\delta > 0$ be such that $2\varepsilon < \eta(\delta)$. If $d_M(x, x') \geq \delta$, then by definition of separation modulus, $\|\Gamma_K(x) - \Gamma_K(x')\| \geq \eta(\delta)$, contradicting $\|\Gamma_K(x) - \Gamma_K(x')\| \leq 2\varepsilon$. Therefore $d_M(x, x') < \delta$. \square

Remark 6.5 (When the condition is (not) informative). If $2\varepsilon \geq \sup_{\delta \in (0, \text{diam}(M)]} \eta(\delta)$, then there may be no δ satisfying $2\varepsilon < \eta(\delta)$ and Proposition 6.4 yields no nontrivial separation guarantee. Interpretationally, this corresponds to prediction being insufficiently accurate (in the uniform sense) to force state separation at any prescribed spatial scale δ .

Corollary 6.6 (Quantitative Separation). *If additionally P is L -Lipschitz on $f(M)$ for some $L > 0$, then:*

$$\|f(x) - f(x')\| \geq \frac{\max\{0, \|\Gamma_K(x) - \Gamma_K(x')\| - 2\varepsilon\}}{L}.$$

6.3 Interpretation and Caveats

Proposition 6.4 is a **deterministic lemma**: low *uniform* prediction error implies approximate injectivity.

Caveat 1: Uniform vs. Expected Error. Training minimizes expected loss under a sampling distribution, not uniform error. The gap between expected and uniform error depends on covering numbers, generalization bounds, and distributional assumptions. We do not analyze this gap here.

Caveat 2: Training Dynamics. Even if low-error solutions exist and correspond to embeddings, we do not analyze whether gradient descent or least squares finds them. The loss landscape for RNNs is complex. Similar considerations would apply in the context of neurobiological RNN training, which involves neuroplasticity mechanisms with the same teleological goal of prediction error minimization. Analyzing convergence guarantees under biologically plausible learning rules remains an important direction for future work.

Interpretation: The proposition explains the *correlation* between prediction quality and embedding quality (as observed by Ostrow et al.): models achieving low prediction error necessarily have approximately injective representations. This is a necessary, not sufficient, condition; it does not prove training reliably finds such solutions.

6.4 Separation Modulus

A (positive) separation modulus exists for any continuous injective map Γ_K on compact M ; for each $\delta > 0$ one may define

$$\eta(\delta) := \inf \left\{ \|\Gamma_K(x) - \Gamma_K(x')\| : d_M(x, x') \geq \delta \right\},$$

and compactness (together with continuity and injectivity) implies $\eta(\delta) > 0$. Stronger, *linear* moduli of the form $\eta(\delta) \geq c\delta$ follow under bi-Lipschitz (or bounded-distortion) hypotheses on Γ_K and its inverse.

7 Discussion

7.1 Summary of Results

Theorem 4.3 establishes that contracting RNNs driven by regular dynamics generically implement C^1 embeddings; Propositions 3.1 and 6.4 characterize bunching conditions and the prediction–separation link.

7.2 Relation to Empirical Findings

The Uribarri–Mindlin [1] and Ostrow et al.[2] studies demonstrated that RNNs trained on chaotic time series learn topologically correct embeddings. Those settings involve strange attractors where bunching, weak generalized synchronization, and fractal-dimension issues are genuinely in play; the regular-dynamics regime treated here avoids these obstructions and therefore admits cleaner guarantees.

However, our results clarify the logical structure:

- Embedding is *guaranteed* (under generic conditions, mild bunching) for regular dynamics.
- Embedding is *observed* (empirically) even for chaotic dynamics, despite weaker mathematical guarantees.
- This suggests a hierarchy of difficulty: if embedding occurs for strange attractors (the hard case), it certainly occurs for limit cycles and tori (the easy case).

The chaotic-attractor findings are *stronger* than what the theory for regular dynamics predicts, suggesting that additional mechanisms (implicit regularization, architectural inductive biases, properties of gradient descent) enforce embedding even when the mathematical conditions are not fully satisfied. Understanding these mechanisms is an important direction for future work.

Remark 7.1 (Periodic Orbit Skeleton and Attractor Compression). For many low-dimensional chaotic (strange) attractors, the unstable periodic orbits (UPOs) form a dense set in the attractor, and the attractor’s topological structure can be characterized by the organization of these orbits via their linking invariants and the associated branched-manifold on which they lie [41]. Notably, Uribarri and Mindlin’s key finding was that trained LSTMs preserved the *topological organization of periodic orbits*, verified by linking number analysis. This suggests that “embedding the strange attractor” may effectively mean embedding its periodic orbit skeleton - which is regular structure.

If so, the distinction between chaotic and regular regimes becomes less sharp than it appears: finite-precision neural systems would naturally smooth chaotic trajectories onto the UPO skeleton, since the fractal fine structure is (i) unpredictable beyond the Lyapunov time, (ii) requires infinite precision to resolve, and (iii) provides no additional predictive benefit. The present framework then characterizes precisely what such compression preserves: the C^1 embedding of the regular skeleton that carries the predictively useful topological information.

7.3 Implications for the State Space Theory of Consciousness

(i) What the mathematics guarantees in the sensory/ESP regime. In the contractive (ESP) setting, generalized synchronization yields a unique invariant graph $f : M \rightarrow \mathbb{R}^N$ (Theorem 2.16) and, under mild bunching, C^1 regularity (Theorem 2.18). In the regular base regimes emphasized here, the bunching requirement is quantitatively mild (Proposition 3.1), and genericity results imply that f is typically a C^1 embedding (Theorem 2.21 and Theorem 4.3). When f is injective, the induced dynamics on the embedded image $f(M)$ are conjugate to ϕ (Theorem 4.3(iii)), so qualitative dynamical invariants of the base (e.g. rotation numbers and winding structure in the quasiperiodic cases) are preserved in the neural representation.

(ii) What this does not address (and why SST still needs additional machinery).

The present synthesis is intentionally restricted to fixed-parameter networks in a contractive regime, which we argued is most plausible for early sensory cortex (Section 2.5). SST’s broader account of consciousness invokes hierarchical integration, gain-modulated competition, and plasticity during processing, including regimes where strict ESP is unlikely to hold (e.g. persistent-activity attractor

dynamics in prefrontal circuits). Those ingredients are therefore not consequences of the present theorems; rather, this paper isolates what the contractive GS/embedding framework can rigorously support as a mathematical substrate for the sensory front-end of SST. Section 6 offers conceptual grounding for why embedding structure may emerge even in non-ESP networks.

(iii) Implications, constraints and empirically testable predictions.

1. The embedding results make the representational content inherently temporal: the state $h_t = f(m_t)$ is equivalent (up to approximation; Proposition 4.6) to a function of a finite delay vector, so the representation encodes trajectory structure rather than a static snapshot.
2. The unfolding argument [42] presents a strong challenge to theories of consciousness and is based on the universal approximation theorem: that any RNN can be unfolded to an equivalent FNN and vice versa. SST’s plasticity-based rebuttal of the unfolding argument ([43]), succinctly stated, is that biological networks change during processing. This rebuttal is independent of the present framework, which assumes fixed parameters. The framework is *compatible with* SST’s process-based rebuttal: if representation constitutively encodes a trajectory rather than a snapshot (per 1), then the temporal structure is not eliminable via unfolding. See [7, 24] for further development of this rebuttal along process-based lines.
3. The dimension bound $N > 2d$ provides a principled capacity constraint: a neural state space of effective dimension N can generically embed dynamics of intrinsic dimension at most $(N-1)/2$, implying that perceptual representations should track low-dimensional dynamical structure and its invariants.
4. Section 6 connects prediction objectives to state separation: low multi-step prediction error forces approximately injective representations (Proposition 6.4), which offers a clean explanation for the empirical correlation between prediction performance and embedding metrics in neural sequence models [2]. Finally, a predictive-processing interpretation remains compatible with these claims: prediction error minimization can be understood as driving circuits toward state-separating, dynamically faithful embeddings, while the agent’s priors determine which environmental structure is treated as “expected” [16, 17].
5. The synchronization relation $f(\phi(x)) = F(f(x), \omega(x))$ identifies the predicted state with the next neural state; the trajectory *is* the prediction. This structural feature is compatible with SST’s identity thesis, which proposes that phenomenal consciousness is constituted by hierarchical DCE processes [7, 24]; the present framework provides mathematical foundations for that proposal without establishing the metaphysical claim itself.

7.4 Limitations

Scope. The synthesis addresses single DCE engines in the sensory ESP regime. SST’s account of consciousness requires hierarchical integration, gain-modulated competition, and meta-representational capacity in prefrontal regions where ESP likely fails. Bridging this sensory/prefrontal gap requires tools beyond the contractive framework assumed here.

Plasticity. The mathematical framework assumes fixed parameters. SST’s process-ontological commitments treat ongoing plasticity as constitutive of conscious computation, not merely implementational. Formalizing this remains open [43].

Other limitations. We do not analyze training dynamics, noise robustness [44], architecture-specific properties, or extension to chaotic attractors. Empirical tests of SST’s predictions (topological preservation, dimension scaling, recurrence-dependence) await development.

7.5 Relation to Other Frameworks

SST intersects with predictive-processing accounts [16, 17], which emphasize prediction, and with ecological psychology [45], which emphasizes resonance to environmental structure. These viewpoints are compatible at the level of this paper: prediction objectives help explain *why* circuits are driven toward state-separating representations, while the GS/embedding framework specifies *when* and *how* contracting recurrent dynamics implement smooth embeddings that preserve dynamical invariants. Whether such embeddings constitute “direct” perception in Gibson’s sense is terminological; mathematically, the key point is that embeddings preserve qualitative structure while encoding trajectory information internally.

8 Conclusion

We have provided a mathematical synthesis establishing that recurrent neural networks satisfying the echo state property, when driven by regular dynamics on circles or tori, generically implement C^1 embeddings of those dynamics. The key insight is to treat the invariant manifold as the base dynamical system, which makes bunching conditions mild and aligns dimension bounds with intrinsic geometry.

For the State Space Theory, this synthesis provides rigorous foundations at the perceptual level. SST proposes that cortical circuits implement delay coordinate embedding through recurrent dynamics, with perceptual representations constituting embeddings of environmental signals into neural state space. The mathematics of generalized synchronization, originally developed for analyzing chaotic systems in reservoir computing, characterizes what such circuits compute: smooth, injective maps that preserve dynamical structure and encode temporal trajectories.

Future work should extend the analysis to stochastic systems and strange attractors, characterize training dynamics, and develop empirical tests of SST’s predictions. The synthesis presented here establishes the mathematical foundations; building on them is the work ahead.

Disclosure of funding: This research received no specific grant from any funding agency in the public, commercial, or not-for-profit sectors.

Conflicts of interest: All authors declare: no support from any organization for the submitted work; no financial relationships with any organizations that might have an interest in the submitted work in the previous three years; no other relationships or activities that could appear to have influenced the submitted work.

Author contributions: All authors meet ICMJE criteria for authorship. Conceptualization: V-OS; Formal Analysis: A-Sel; Writing (Original Draft): All authors; Writing (Review & Editing): All authors.

Acknowledgements: The authors would like to thank their respective universities for their generous support of the authors' time.

Declaration of generative AI and AI-assisted technologies in the writing process: During the preparation of this work the author(s) used OpenAI ChatGPT, Anthropic Claude, and Google Gemini models in order to polish written content, assist with the formatting of proofs in L^AT_EX, and assist with the coding of TikZ figures in L^AT_EX. After using this tool/service, the authors reviewed and edited the content. The authors take full responsibility for the manuscript in its entirety. Citations were manually retrieved from traditional sources (e.g., PubMed).

Data Availability Statement: This is a theoretical synthesis paper. No new data were generated or analyzed. There is no empirical data or code associated with this article.

References

- [1] G Uribarri and G. B Mindlin. Dynamical time series embeddings in recurrent neural networks. *Chaos, Solitons & Fractals*, 154:111612, 2022. doi: 10.1016/j.chaos.2021.111612.
- [2] Mitchell Ostrow, Adam Eisen, and Ila Fiete. Delay embedding theory of neural sequence models. *International Conference on Machine Learning (ICML) workshop on Next Generation Sequence Modeling*, 2024. URL <https://arxiv.org/abs/2406.11993v1>.
- [3] A. G Hart. Generic and isometric embeddings in reservoir computers. *Chaos*, 35:111103, 2025. doi: 10.1063/5.0288408.
- [4] F Takens. Detecting strange attractors in turbulence. In D. Rand and L.-S. Young, editors, *Dynamical Systems and Turbulence, Warwick 1980*, volume 898 of *Lecture Notes in Mathematics*, pages 366–381. Springer, 1981.
- [5] T Sauer, J. A Yorke, and M Casdagli. Embedology. *Journal of Statistical Physics*, 65(3–4):579–616, 1991. doi: 10.1007/BF01053745.
- [6] Vikas O'Reilly-Shah. Delay coordinate embedding as neuronally implemented information processing: The state space theory of consciousness. *Journal of Consciousness Studies*, 32(1–2):132–164, 2025.
- [7] Vikas O'Reilly-Shah. State space theory as a unifying framework for consciousness. *Nonlinear Dynamics, Psychology, and Life Sciences*, forthcoming/scheduled, April 2026. URL <https://philpapers.org/rec/ORESST>.
- [8] M Zago, J McIntyre, P Senot, and F Lacquaniti. Visuo-motor coordination and internal models for object interception. *Experimental Brain Research*, 192(4):571–604, 2009. doi: 10.1007/s00221-008-1691-3.
- [9] J. A. S Kelso. *Dynamic patterns: The self-organization of brain and behavior*. MIT Press, 1995.
- [10] S Vyas, M. D Golub, D Sussillo, and K. V Shenoy. Computation through neural population dynamics. *Annual Review of Neuroscience*, 43:249–275, 2020. doi: 10.1146/annurev-neuro-092619-094115.
- [11] E. L Saltzman and K. G Munhall. A dynamical approach to gestural patterning in speech production. *Ecological Psychology*, 1(4):333–382, 1989.
- [12] R. F Port. Meter and speech. *Journal of Phonetics*, 31(3–4):599–611, 2003.
- [13] E. W Large and J. F Kolen. Resonance and the perception of musical meter. *Connection Science*, 6(2–3):177–208, 1994.
- [14] B. A Wandell. *Foundations of vision*. Sinauer Associates, 1995.
- [15] D. H Brainard and W. T Freeman. Bayesian color constancy. *Journal of the Optical Society of America A*, 14(7):1393–1411, 1997.
- [16] K Friston. The free-energy principle: A unified brain theory? *Nature Reviews Neuroscience*, 11(2):127–138, 2010. doi: 10.1038/nrn2787.

[17] A Clark. Whatever next? predictive brains, situated agents, and the future of cognitive science. *Behavioral and Brain Sciences*, 36(3):181–204, 2013.

[18] M. M Churchland, J. P Cunningham, M. T Kaufman, J. D Foster, P Nuyujukian, S. I Ryu, and K. V Shenoy. Neural population dynamics during reaching. *Nature*, 487(7405):51–56, 2012. doi: 10.1038/nature11129.

[19] N Sadato, A Pascual-Leone, J Grafman, V Ibañez, M.-P Deiber, G Dold, and M Hallett. Activation of the primary visual cortex by Braille reading in blind subjects. *Nature*, 380(6574):526–528, 1996.

[20] L. G Cohen, P Celnik, A Pascual-Leone, B Corwell, L Faiz, J Dambrosia, M Honda, N Sadato, C Gerloff, M. D Catalá, and M Hallett. Functional relevance of cross-modal plasticity in blind humans. *Nature*, 389(6647):180–183, 1997.

[21] K Siuda-Krzywicka, A Marchewka, M. W Śliwińska, A Amedi, and M Szwed. Massive cortical reorganization in sighted Braille readers. *eLife*, 5:e10762, 2016. doi: 10.7554/eLife.10762.

[22] A. N Whitehead. *Process and Reality*. Macmillan, 1929.

[23] E. G Husserl. *On the phenomenology of the consciousness of internal time (1893-1917) (J. B. Brough, Trans.)*. Kluwer Academic Publishers, 1991.

[24] Vikas O'Reilly-Shah. Computational dynamic monism: Process metaphysics for the state space theory of consciousness. *SSRN Electronic Journal (PREPRINT)*, dec 2025. doi: 10.2139/ssrn.6042716. URL <https://ssrn.com/abstract=6042716>.

[25] J Stark. Delay embeddings for forced systems. i. deterministic forcing. *Journal of Nonlinear Science*, 9(2):255–332, 1999.

[26] A Hart, J Hook, and J Dawes. Embedding and approximation theorems for echo state networks. *Neural Networks*, 128:234–247, 2020.

[27] J Stark. Regularity of invariant graphs for forced systems. *Ergodic Theory and Dynamical Systems*, 19(1):155–199, 1999.

[28] J. M Beggs and D Plenz. Neuronal avalanches in neocortical circuits. *Journal of Neuroscience*, 23(35):11167–11177, 2003. doi: 10.1523/JNEUROSCI.23-35-11167.2003.

[29] N Bertschinger and T Natschläger. Real-time computation at the edge of chaos in recurrent neural networks. *Neural Computation*, 16(7):1413–1436, 2004.

[30] S Funahashi, C. J Bruce, and P. S Goldman-Rakic. Mnemonic coding of visual space in the monkey's dorsolateral prefrontal cortex. *Journal of Neurophysiology*, 61(2):331–349, 1989.

[31] X.-J Wang. Synaptic reverberation underlying mnemonic persistent activity. *Trends in Neurosciences*, 24(8):455–463, 2001. doi: 10.1016/S0166-2236(00)01868-3.

[32] H. K Inagaki, L Fontolan, S Romani, and K Svoboda. Discrete attractor dynamics underlies persistent activity in the frontal cortex. *Nature*, 566(7743):212–217, 2019. doi: 10.1038/s41586-018-0783-x.

[33] J. D Murray, A Bernacchia, D. J Freedman, R Romo, J. D Wallis, X Cai, C Padoa-Schioppa, T Pasternak, H Seo, D Lee, and X.-J Wang. A hierarchy of intrinsic timescales across primate cortex. *Nature Neuroscience*, 17(12):1661–1663, 2014.

[34] G Manjunath and H Jaeger. Echo state property linked to an input: Exploring a fundamental characteristic of recurrent neural networks. *Neural Computation*, 25(3):671–696, 2013. doi: 10.1162/NECO_a_00489.

[35] I. B Yildiz, H Jaeger, and S. J Kiebel. Re-visiting the echo state property. *Neural Networks*, 35:1–9, 2012. doi: 10.1016/j.neunet.2012.07.005.

[36] D Nikolić, S Häusler, W Singer, and W Maass. Distributed fading memory for stimulus properties in the primary visual cortex. *PLOS Biology*, 7(12):e1000260, 2009. doi: 10.1371/journal.pbio.1000260.

[37] G Hennequin, Y Ahmadian, D. B Rubin, M Lengyel, and K. D Miller. The dynamical regime of sensory cortex: Stable dynamics around a single stimulus-tuned attractor account for patterns of noise variability. *Neuron*, 98(4):846–860, 2018.

[38] C Stringer, M Michaelos, D Tsyboulski, S. E Lindo, and M Pachitariu. High-dimensional geometry of population responses in visual cortex. *Nature*, 571(7765):361–365, 2019. doi: 10.1038/s41586-019-1346-5.

[39] G Keller, H. H Jafri, and R Ramaswamy. Nature of weak generalized synchronization in chaotically driven maps. *Physical Review E*, 87(4):042913, 2013.

[40] J. D Murray, A Bernacchia, N. A Roy, C Constantinidis, R Romo, and X.-J Wang. Stable population coding for working memory coexists with heterogeneous neural dynamics in prefrontal cortex. *Proceedings of the National Academy of Sciences*, 114(2):394–399, 2017.

[41] Robert Gilmore and Christophe Letellier. *The symmetry of chaos*. Oxford University Press, New York, NY, May 2007.

[42] A Doerig, A Schuriger, K Hess, and M. H Herzog. The unfolding argument: Why IIT and other causal structure theories cannot explain consciousness. *Consciousness and Cognition*, 72:49–59, 2019. doi: 10.1016/j.concog.2019.03.003.

[43] Vikas O'Reilly-Shah, Alessandro Selvitella, and Aaron Schuriger. A caveat regarding the unfolding argument: Implications of plasticity for computational theories of consciousness. *bioRxiv (PREPRINT)*, 2025. doi: 10.1101/2025.11.04.686457. URL <https://www.biorxiv.org/content/early/2025/11/05/2025.11.04.686457.1>.

[44] J Stark, D. S Broomhead, M. E Davies, and J Huke. Delay embeddings for forced systems. ii. stochastic forcing. *Journal of Nonlinear Science*, 13(6):519–577, 2003.

[45] J. J Gibson. *The ecological approach to visual perception*. Houghton Mifflin, 1979.